

# Microarrays of lentiviruses for gene function screens in immortalized and primary cells

Steve N Bailey, Siraj M Ali, Anne E Carpenter, Caitlin O Higgins & David M Sabatini

**Here we describe lentivirus-infected cell microarrays for the high-throughput screening of gene function in mammalian cells. To create these arrays, we cultured mammalian cells on glass slides 'printed' with lentiviruses pseudotyped as vesicular stomatitis virus glycoprotein, which encode short hairpin RNA or cDNA. Cells that land on the printed 'features' become infected with lentivirus, creating a living array of stably transduced cell clusters within a monolayer of uninfected cells. The small size of the features of the microarrays (300  $\mu\text{m}$  in diameter) allows high-density spotting of lentivirus, permitting thousands of distinct parallel infections on a single glass slide. Because lentiviruses have a wide cellular tropism, including primary cells, lentivirus-infected cell microarrays can be used as a platform for high-throughput screening in a variety of cell types.**

RNA interference (RNAi) technology allows for loss-of-function studies in mammalian cells without the need for germline inactivation of the gene being studied<sup>1</sup>. A robust, inexpensive RNAi-based high-throughput screening platform would facilitate genome-scale loss-of-function studies in mammalian cells. *Drosophila* cell-based microarrays are effective for high-throughput RNAi-based loss-of-function screens, but can only be used to study cell-biological phenomena that take place in *drosophila* cell lines. To enable similar studies in mammalian cells, several groups have developed cell-based microarrays using small interfering RNA or DNA plasmids. However, such microarrays rely on conventional transfection methods and thus are unlikely to be broadly compatible with many different cell types<sup>2–6</sup>.

Because lentiviruses pseudotyped as vesicular stomatitis virus glycoprotein (VSV-G) infect a wide variety of mammalian cells with high efficiency<sup>7</sup>, they avoid many of the limitations of transfection for introducing over- or underexpression cassettes into cells. Such lentiviruses can be used to overexpress cDNA and to express short hairpin RNA (shRNA) that silences gene expression through RNAi<sup>8,9</sup>. Notably, lentiviruses can infect nondividing cells, a capacity that is particularly useful for the study of certain primary cell types<sup>7</sup>.

Here we describe a new type of cell-based microarray whose features include clusters of mammalian cells, each transduced with a single type of lentivirus. We refer to these as lentivirus-infected

cell microarrays (LICMs). With these microarrays, we have obtained robust and localized infection of mammalian cells with lentiviruses containing overexpression cassettes or RNAi cassettes. This technology provides a platform for loss-of-function and overexpression screens in a broad range of mammalian cell types.

## RESULTS

### Development of the LCIM

The 'features' of LICMs comprise clusters of mammalian cells, each infected with a distinct lentivirus and surrounded by a monolayer of uninfected cells. To make the microarrays, we 'print' on a coated glass slide nanoliter volumes of solutions containing concentrated lentivirus. We place dried printed slides in a Petri dish and add adherent mammalian cells in media. After an incubation of typically 72–96 h, the LICM forms and the cells can be fixed and processed with conventional cell-based assay methods, such as immunofluorescence. Each cell cluster on the microarray is then imaged with automated microscopy and analyzed for cellular phenotypes of interest. To demonstrate this technology, we printed a microarray with 300 features, each containing either a lentivirus encoding green fluorescent protein (GFP) or an shRNA targeting human lamin A/C<sup>8</sup>. We seeded  $2 \times 10^6$  HeLa cells onto the array and, after 72 h, processed it and imaged cells for expression of GFP or lamin A/C and DNA content. In a pattern matching that of the lentivirus-containing features on the array, cell clusters expressing GFP or deficient in lamin A/C were clearly visible (**Fig. 1a**). Each cluster was approximately 250  $\mu\text{m}$  in diameter and contained about 150 cells. At this 'feature density', 5,000 different lentiviruses can be printed on a single slide.

In the example above, we printed the two different lentiviruses in an alternating pattern to assess whether cells on one feature would become infected with viruses from vicinal features. This does not seem to be the case, because cells on the GFP-lentivirus features had high levels of green fluorescence but expressed normal amounts of lamin A/C (**Fig. 1b**). Conversely, the cells on features printed with the lamin A/C shRNA lentivirus had a fivefold reduction in lamin A/C expression compared with cells growing either on nonprinted areas of the slide or on the GFP-lentivirus features. The number of cells with 'knockdown' of lamin A/C expression was six times greater on features printed with the lamin A/C

Whitehead Institute for Biomedical Research and Massachusetts Institute of Technology Department of Biology, Nine Cambridge Center, Cambridge, Massachusetts 02142, USA. Broad Institute, 320 Charles Street, Cambridge, Massachusetts 02141, USA. Correspondence should be addressed to D.M.S. (sabatini@wi.mit.edu).

RECEIVED 3 OCTOBER 2005; ACCEPTED 19 DECEMBER 2005; PUBLISHED ONLINE 23 JANUARY 2006; DOI:10.1038/NMETH848

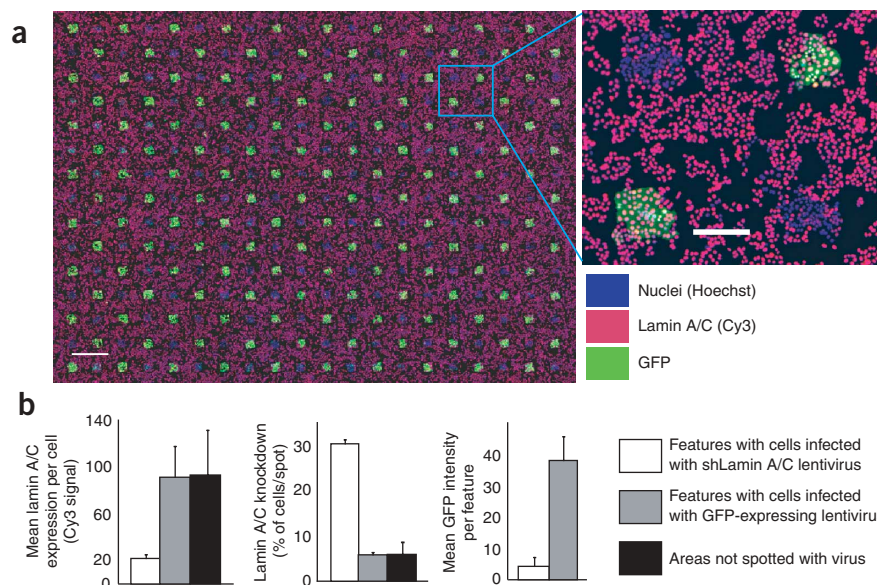


**Figure 1** | LICMs made with two different types of lentiviruses. **(a)** Microarray of 300 features printed with lentiviruses expressing either GFP or shRNA targeting lamin A/C in an alternating pattern, and seeded with HeLa cells. Hoechst staining shows nuclei (blue), anti-lamin A/C immunofluorescence shows lamin A/C (red) and GFP fluorescence is green. Right, higher magnification image of four features from the array (boxed at left). Scale bars, 1 mm (left) and 200  $\mu\text{m}$  (right). **(b)** Quantification of GFP and lamin A/C expression in features of the array and nonspotted control areas. For lamin A/C, we quantified both mean expression per cell (left; arbitrary units) and percent of cells in a feature with reduced lamin A/C expression (knockdown; middle). For GFP, we quantified mean GFP expression per feature (right; arbitrary units). Measurements are based on  $n = 160$ . Cy3, indocarbocyanine; shLamin A/C, shRNA targeting lamin A/C (see **Supplementary Note**).

shRNA lentivirus than on the GFP-lentivirus features or in feature-sized nonprinted areas of the slide. Our quantitative analysis suggests that features printed with lentiviruses infect small clusters of cells in a local, virus-specific way. In addition, our example demonstrates the use of overexpression and shRNA lentiviruses on the same microarray.

### Use of primary dividing and nondividing cells on LICMs

Having demonstrated the feasibility of LICMs, we explored their possible uses and limitations in more detail. We first tested the

effect of printing different amounts of lentivirus in each spot. The typical titer of a printed lentiviral solution is  $1 \times 10^9$  infectious units (IFU)/ml. In each feature we deposit about 3.9 nl of solution or 3,900 IFU/feature. Each feature has about 150 cells and thus roughly 26 IFU/cell. We printed twofold serial dilutions of a solution containing GFP-encoding lentivirus (initial titer,  $2 \times 10^9$  IFU/ml) on multiple arrays and quantified the subsequent level of GFP expression in the cells growing on those features. As seen with conventional lentiviral infections, the amount of lentivirus deposited in each spot was proportional to the magnitude of the

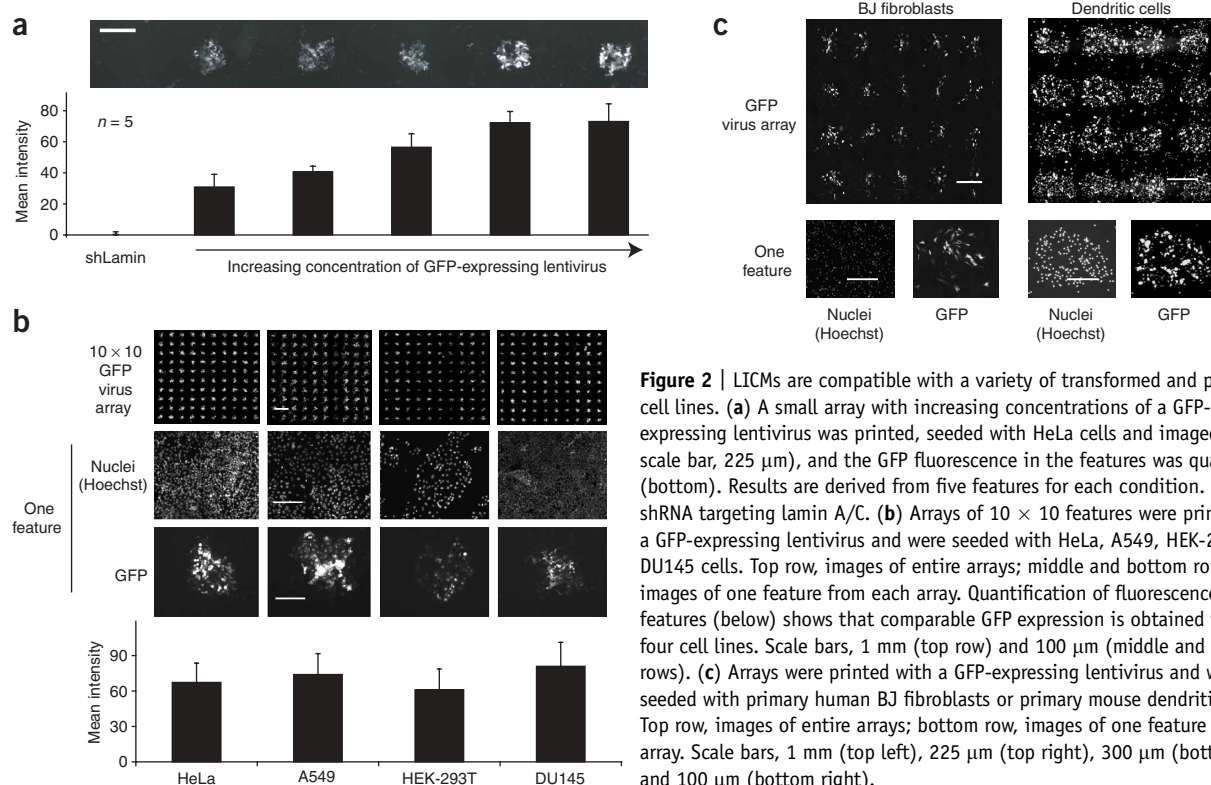


**Figure 2** | LICMs are compatible with a variety of transformed and primary cell lines. **(a)** A small array with increasing concentrations of a GFP-expressing lentivirus was printed, seeded with HeLa cells and imaged (top; scale bar, 225  $\mu\text{m}$ ), and the GFP fluorescence in the features was quantified (bottom). Results are derived from five features for each condition. shLamin, shRNA targeting lamin A/C. **(b)** Arrays of 10  $\times$  10 features were printed with a GFP-expressing lentivirus and were seeded with HeLa, A549, HEK-293T or DU145 cells. Top row, images of entire arrays; middle and bottom rows, images of one feature from each array. Quantification of fluorescence in features (below) shows that comparable GFP expression is obtained with the four cell lines. Scale bars, 1 mm (top row) and 100  $\mu\text{m}$  (middle and bottom rows). **(c)** Arrays were printed with a GFP-expressing lentivirus and were seeded with primary human BJ fibroblasts or primary mouse dendritic cells. Top row, images of entire arrays; bottom row, images of one feature from each array. Scale bars, 1 mm (top left), 225  $\mu\text{m}$  (top right), 300  $\mu\text{m}$  (bottom left) and 100  $\mu\text{m}$  (bottom right).

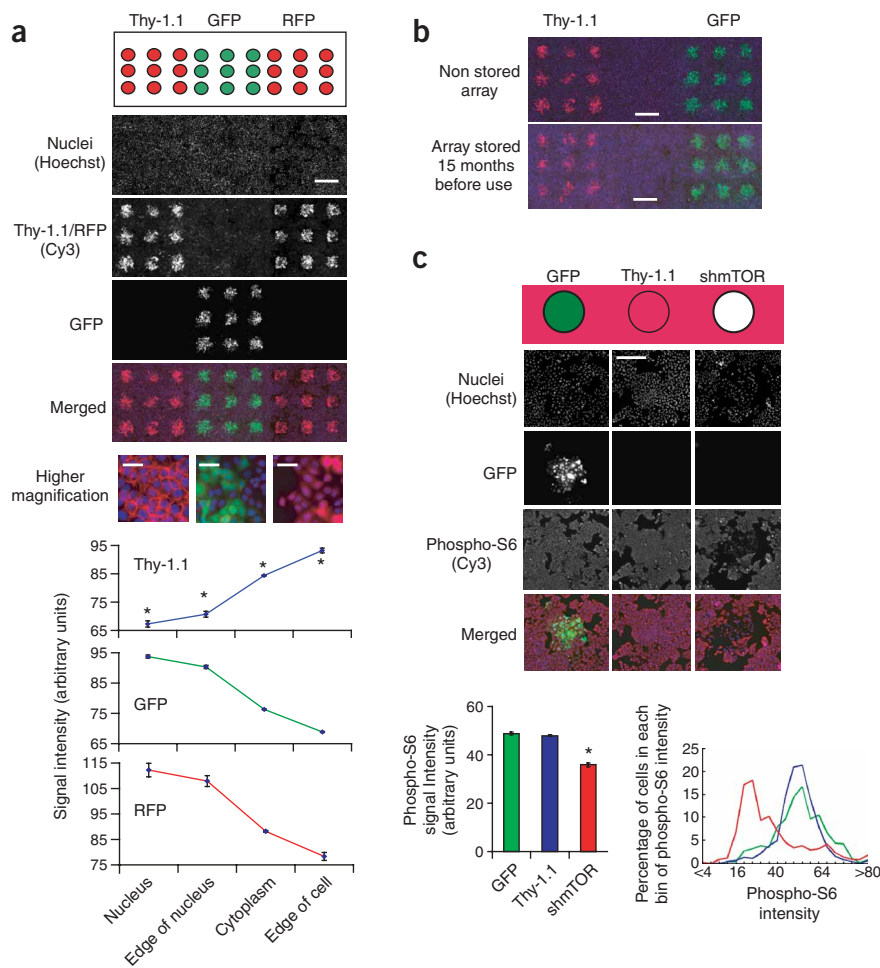


**Figure 3** | LICMs are compatible with the detection of complex phenotypes. **(a)** These  $3 \times 3$  arrays were printed with viruses using different promoters to overexpress GFP, RFP and Thy-1.1. Hoechst staining shows nuclei; immunofluorescence with antibody to Thy-1.1 shows membrane-localized Thy-1.1 (red); GFP fluorescence is green; RFP fluorescence is also red. Each feature was also imaged at high magnification (bottom row, representative images). Scale bars,  $450 \mu\text{m}$  (main images) and  $25 \mu\text{m}$  (higher magnification). These images were analyzed to assess the subcellular distribution of each protein (see **Supplementary Note**). Error bars, s.e.m.; \*,  $P < 0.01$ , subcellular localization of Thy-1.1 versus GFP and RFP. **(b)** Experiments with arrays similar to that in **a**, assayed on the day of printing (top) or after storage for 15 months at  $-80^\circ\text{C}$  (bottom). **(c)** Arrays were printed with lentiviruses expressing GFP or Thy-1.1 or an shRNA targeting mTOR (shmTOR). Single features from the array are presented. Scale bar,  $150 \mu\text{m}$ . Hoechst staining shows nuclei; immunofluorescence with antibody to phosphorylated S6 (Phospho-S6) shows mTOR pathway activity (red); and GFP fluorescence is green. For quantification of S6 phosphorylation, images of six features for each sample type (GFP, Thy-1.1 and shmTOR) were analyzed. For each feature, the mean fluorescence intensity of phospho-S6 staining in the cytoplasm was measured for every cell (see **Supplementary Note**). Bottom left, population-averaged data. Error bars, s.e.m.; \*,  $P < 0.01$ , versus Thy-1.1 as a control. Bottom right, cells from those populations were placed into bins based on their mean intensity values: red line, shmTOR; green line, GFP; blue line, Thy-1.1.

phenotypic change seen in cells growing on the corresponding feature (**Fig. 2a**).

Viruses pseudotyped as VSV-G readily infect many different mammalian cell types<sup>7</sup>. To demonstrate this capacity of lentiviruses in the array format, we printed four identical, 100-feature arrays of the GFP-encoding lentivirus and cultured a different cell type on each (**Fig. 2b**). Although the average GFP expression was highest in A549 and DU145 cells, all four cell types tested had levels of GFP expression that were well above the background of uninfected cells. This result demonstrates how LICMs can be used with commonly used adherent, cultured cell lines, both transformed and nontransformed. To demonstrate the compatibility of LICMs with primary mammalian cells, we cultured primary dividing human BJ fibroblasts or primary nondividing bone marrow-derived mouse dendritic cells on an array printed with lentivirus containing a GFP-overexpression cassette (**Fig. 2c**). The arrays produced grids of GFP-expressing features in the printed pattern, showing that the microarrays are compatible with nondividing and dividing primary cells and that cell division is not necessary for the formation of LICMs.

#### Quantification of high-content cellular phenotypes

We have demonstrated that LICMs are compatible with overexpression and shRNA-mediated 'knockdown' with lentiviruses. To ensure that this functionality is not specific to the lentiviral vectors or cDNAs used, we tested several different lentiviruses in

the array format. We printed small grids with lentiviruses containing overexpression cassettes of GFP driven by the phosphoglycerate kinase promoter derived from transfection using the plasmid LKO.1, red fluorescent protein (RFP) driven by the ubiquitin C promoter derived from transfection using the plasmid Lentilox 3.7, or Thy-1.1 (CD90) driven by the ubiquitin C promoter derived from transfection using the plasmid LKO.2 (refs. 8,9; **Fig. 3a**). All three lentiviruses produced localized cell clusters expressing only the expected proteins, suggesting that the microarrays are compatible with a wide variety of promoters for gene overexpression and distinct viral 'backbones'. At high magnification, the membrane-targeted localization of Thy-1.1 was visibly distinguishable from the subcellular distribution of RFP and GFP (**Fig. 3a**, bottom images). We also measured the membrane localization of Thy-1.1 quantitatively and automatically on an individual cell basis (**Fig. 3a**, graphs) using the CellProfiler image analysis software developed in our laboratory ([www.cellprofiler.org](http://www.cellprofiler.org)). Our results suggest that lentiviruses printed in LICM features preserve the characteristics of VSV-G lentiviruses, including high efficiency infection of transformed and primary mammalian cells and transduction of shRNA<sup>7</sup>.

For use in a screening format, the arrays must be stable and durable. We printed multiple copies of the microarrays described above and stored the replicate arrays at  $-80^\circ\text{C}$  for 15 months. After storage, we thawed the slides, then seeded and analyzed them in the same way as the freshly assayed arrays. The similarity of

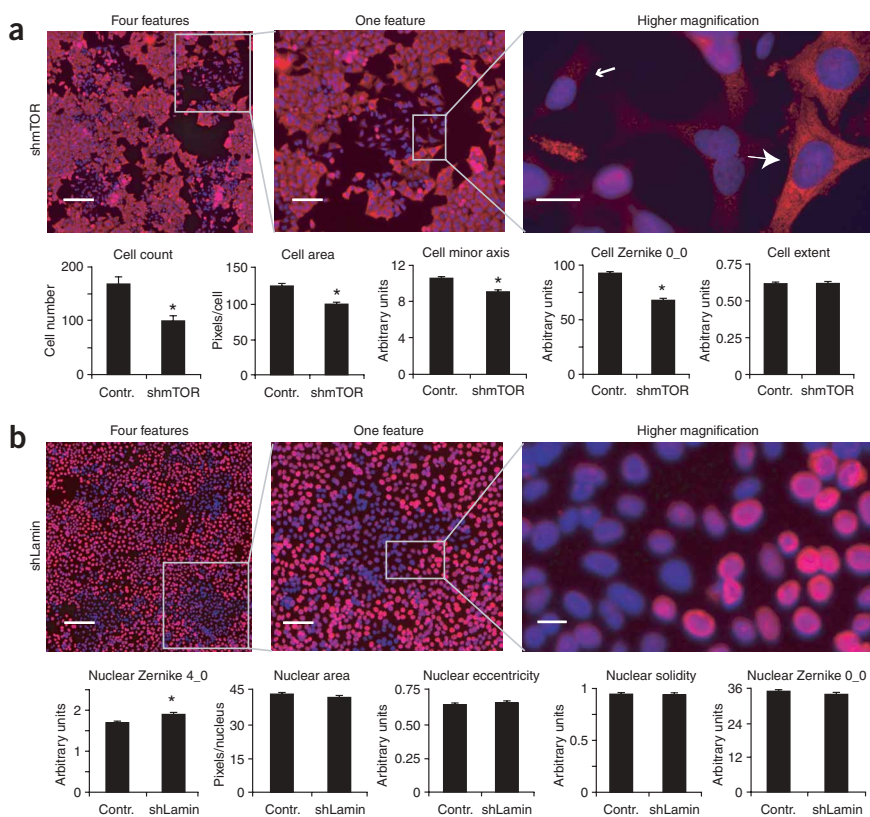


**Figure 4** | Complex cellular phenotypes can be detected by automated image analysis of LICM features. (a,b) Arrays printed with lentiviruses expressing shRNA targeting mTOR or lamin A/C were seeded with HeLa cells and processed for phospho-S6 (a) or lamin A/C (b) immunofluorescence. Hoechst staining shows nuclei (blue); immunofluorescence with antibody to phosphorylated S6 and antibody to lamin A/C are cytoplasmic and nuclear stains, respectively (red). Scale bars, 150  $\mu\text{m}$  (four features), 40  $\mu\text{m}$  (one feature) and 10  $\mu\text{m}$  (higher magnification). The small arrow in a indicates a small cell with a decrease in phospho-S6 staining; the large arrow indicates an unaffected cell. Automated shape and size measurements were obtained for every cell in the shmTOR features and every nucleus in the shLamin features (see **Supplementary Note**). Graphs present the population-averaged data for several of these measurements. Error bars, s.e.m.; \*,  $P < 0.01$ . Contr. (control), Thy1.1 overexpression (a) or GFP overexpression (b). See **Supplementary Note** for a full description of the automated image analysis protocols.

the results obtained with fresh and stored arrays suggests that the printed slides can be stored for extended periods of time before use (Fig. 3b).

We also demonstrated that LICMs can be used to detect cellular phenotypes caused by the ‘knockdown’ of an endogenous gene. We seeded HeLa cells onto an array printed with a lentivirus encoding an shRNA targeting human mTOR, a central regulator of cell growth (cell size) and proliferation (cell number)<sup>10</sup>, in addition to features printed with lentiviruses overexpressing GFP or Thy-1.1. We assayed mTOR activity through the phosphorylation state of its ‘downstream’ effector, the ribosomal protein S6 (Fig. 3c). The cells in the features printed with lentivirus encoding shRNA targeting mTOR had a visually obvious reduction in S6 phosphorylation, which was unaffected in cells in the features with overexpression of Thy-1.1 or GFP. Quantitative image analysis using CellProfiler as described in the **Supplementary Note** online confirmed these results for the cell population (Fig. 3c, bar graphs) and on a per-cell basis (Fig. 3c, histograms).

Finally, we showed that LICMs are compatible with the detection of cellular phenotypes that are not exclusively based on fluorescence

intensity. We measured 39 size and shape parameters of the cytoplasm and nuclei of HeLa cells growing on features printed with lentiviruses expressing shRNA targeting mTOR or lamin A/C. Some but not all of the parameters were affected by ‘knockdown’ of mTOR or lamin A/C (subset, Fig. 4). For example, features printed with lentivirus encoding shRNA targeting mTOR had fewer and smaller cells than did features printed with a control lentivirus, consistent with the known involvement of mTOR in cell size control<sup>10</sup>. Some (for example, Zernike 0\_0) but not all (for example, extent) cell shape parameters were also affected by ‘knockdown’ of mTOR (Fig. 4a). Cells in features printed with lentivirus encoding shRNA targeting lamin A/C showed a change only in the Zernike 4\_0 shape parameter of the cell nucleus without an effect on nuclear area or eccentricity (Fig. 4b).

## DISCUSSION

Like other cell-based microarray formats, LICMs have certain advantages over microtiter plate-based screening methods. We print the microarrays on modified glass slides, which yields better image quality for cellular assays than do plates with polystyrene bottoms. The arrays are compatible with the automated detection of ‘high-content phenotypes’, such as the subcellular localization of the Thy-1.1 membrane protein and the size reduction of cells depleted of mTOR. The scale of LICMs also lends itself to ‘savings’ in the number of cells required for a screen. A screen of 5,000 viruses using 384-well

microtiter plates requires about 13 plates and, depending on the cell type, at least  $10 \times 10^6$  cells. At feature densities similar to those used in Figure 1a, 5,000 different viruses can be screened on a single slide using far fewer cells, an important characteristic for primary cells that may be difficult to obtain.

Other cell-based microarray methods use plasmids or small interfering RNA to achieve overexpression or transient ‘knockdown’<sup>2–6,11</sup>. Here, we have demonstrated the ability to do both using stable lentiviral transduction<sup>8</sup>, highlighting the flexibility of LICM technology. Moreover, once printed, the arrays are compatible with a variety of cell types, including primary nondividing cells. We strongly suspect that the format will be adaptable to other viruses pseudotyped as VSV-G, such as Moloney retroviruses. The microarrays may also be compatible with other stable viral pseudotypes, but this remains to be tested.

The main hurdle for adapting LICM to genome-wide loss-of-function screens is the requirement for high-titer virus obtained by concentrating virus-containing supernatants. Ultracentrifugation is time consuming and difficult to automate, but advances in the generation of higher-titer lentiviral supernatants are likely.

In the mean time, the production and screening of focused lentiviral libraries (such as the genes encoding the 'kinome') is practical, allowing the immediate application of LICMs to many cell biology problems.

## METHODS

**Materials.** We obtained immunofluorescence reagents from the following sources and used them at the dilutions in parentheses: mouse monoclonal antibody to lamin A/C (636; 1:500 dilution; Santa Cruz Biotechnology), secondary antibody to mouse–indocarbocyanine (1:1,000 dilution; Jackson Laboratories), antibody to Thy-1–biotin (1:500 dilution; Pharmingen), streptavidin–indocarbocyanine secondary antibody (1:1,000 dilution; Pharmingen), antibody to phosphorylated S6 (ser240/4; 1:500 dilution; Cell Signaling) and Hoechst 33342 (1:10,000 dilution; Molecular Probes). We used the following lentivirus plasmids: PRRL phosphoglycerate kinase–GFP<sup>8</sup>; LKO.1 puro encoding lamin A/C or mTOR shRNA<sup>12</sup>; Lentilox 3.7 CMV-RFP (C. Dillon); and LKO.3 encoding mouse Thy-1.1 (N. Hacohen).

**Lentivirus production.** To generate lentiviruses, we seeded  $6 \times 10^6$  HEK293T cells in 15-cm dishes and, after 48 h, cotransfected the cells with Fugene 6 using 9  $\mu$ g lentiviral plasmid, 6  $\mu$ g Delta VPR 8.9 and 3  $\mu$ g VSV-G<sup>13</sup>. After 24 h, we removed the virus-containing supernatant, filtered it through a 0.45- $\mu$ m cellulose acetate filter and concentrated it by ultracentrifugation at 23,000 r.p.m. in an sw28 rotor in a Beckman ultracentrifuge for 1.5 h (ref. 7). After ultracentrifugation, we resuspended viral pellets in microarray printing solution (0.4 M HEPES, pH adjusted to 7.4 with KOH, 12.5 mg/ml of Trehalose (625625; Calbiochem), 6  $\mu$ g/ml of protamine sulfate (P4020; Sigma) and 1.23 M KCL (3911; Sigma)). We stored concentrated lentivirus at  $-80^\circ\text{C}$  until use.

**Microarray printing.** We used a microarraying robot (Pixsys 5500; Genomic Solutions) with SMP10 pins (Arrayit SMP10; Telechem) to deposit viral solutions on glass slides coated with  $\gamma$ -amino propyl silane (UltraGAPS; 40015; Corning). We used UltraGAPS slides because the surface allowed for the printing of small, well-formed spots and they were compatible with cell culture. Before printing the microarray, we loaded 20  $\mu$ l of viral solution into a round-bottomed, 384-well polypropylene microtiter plate and centrifuged it at 1,000 r.p.m. for 30 s. We did all printing at  $23^\circ\text{C}$  with 55% humidity. The titer of a typical concentrated virus solution is roughly  $1 \times 10^9$  IFU/ml. An SMP10 pin deposits about 3.9 nl of solution to generate spots with a diameter of 200–300  $\mu$ m. After printing, we stored the slides at  $-80^\circ\text{C}$  in sealed airtight bags. In the experiments in **Figures 1, 2a, 2b** and **3**, the center-to-center distance between features was 500  $\mu$ m. In **Figure 2c**, the center-to-center distance between features was 1.5 mm and 500  $\mu$ m for the arrays seeded with the very large BJ fibroblasts and mouse dendritic cells, respectively.

**Lentivirus microarray seeding.** We desiccated stored arrays at  $25^\circ\text{C}$  for 1 h before use. All slides were then 'blocked' for exactly 30 min at  $25^\circ\text{C}$  in a 15-cm dish in Dulbecco's modified Eagle's medium with 10% inactivated fetal calf serum. During the blocking, the slides were positioned so that the printed area on the slide was face down and was not in contact with anything other than the media. After blocking, slides were placed 'array side up' in a

100-mm  $\times$  100-mm  $\times$  10-mm square tissue culture dish. We used actively growing mammalian cells in 25 ml of culture medium (A549 cells: Dulbecco's modified Eagle's medium with 10% fetal bovine serum, 50 units/ml of penicillin and 50  $\mu$ g/ml of streptomycin; HeLa, HEK-293T, DU145 and BJ fibroblasts: Dulbecco's modified Eagle's medium with 10% inactivated fetal calf serum, 50 units/ml of penicillin and 50  $\mu$ g/ml of streptomycin) for seeding the arrays. We incubated seeded arrays at  $37^\circ\text{C}$  in an atmosphere of 5%  $\text{CO}_2$ . For **Figure 2c**, we seeded arrays with  $20 \times 10^6$  human BJ fibroblasts, followed by incubation for 72 h, or seeded arrays with  $1.6 \times 10^6$  mouse dendritic cells, followed by incubation for 92 h. We placed mouse dendritic cells on the slide as a loosely attached aggregate at day 6 after purification from bone marrow<sup>14</sup>. This loosely attached aggregate then released mature, nonproliferating dendritic cells as a final stage of development. For the experiments in **Figures 1, 2a, 3** and **4**, we seeded arrays with  $20 \times 10^6$  HeLa cells and incubated for 72 h. After culture for the specified amount of time, we removed slides from media and fixed them for 20 min at  $25^\circ\text{C}$  in 3.7% paraformaldehyde plus 4% sucrose in PBS.

**Immunofluorescence.** After fixation, we probed cells with primary and secondary antibodies as described<sup>12</sup>.

**Image capture and analysis.** We captured images of arrays with an Axiovert 200 microscope (Carl Zeiss) and analyzed them with custom software designed on the KS400 platform for all figures. Photos of large arrays were captured at  $\times 50$  magnification, images of single features were captured at  $\times 100$  and the image of the feature containing lentivirus expressing an shRNA targeting mTOR was captured at  $\times 400$ . For **Figures 3** and **4**, we used CellProfiler image analysis software developed in our laboratory (<http://www.cellprofiler.org>). See **Supplementary Note** for a full description of the image analysis protocols used.

*Note: Supplementary information is available on the Nature Methods website.*

## ACKNOWLEDGMENTS

We thank S.A. Stewart (Washington University; St. Louis, Missouri) for the gift of LKO.1 puro; C. Dillon (Massachusetts Institute of Technology, Cambridge, Massachusetts) for the gift of Lentilox 3.7-CMV-RFP; and N. Hacohen (Massachusetts General Hospital; Boston, Massachusetts) for the gift of LKO.3 Thy-1.1 and primary mouse dendritic cells. A.E.C. is a Novartis fellow of the Life Sciences Research Foundation; S.M.A. is a Howard Hughes Medical Institute predoctoral fellow. This work was supported by funds from the Whitehead Institute and Pew Charitable Trusts.

## COMPETING INTERESTS STATEMENT

The authors declare that they have no competing financial interests.

Published online at <http://www.nature.com/naturemethods/>  
Reprints and permissions information is available online at  
<http://npg.nature.com/reprintsandpermissions/>

1. Brummelkamp, T.R. & Bernards, R. New tools for functional mammalian cancer genetics. *Nat. Rev. Cancer* **3**, 781–789 (2003).
2. Ziauddin, J. & Sabatini, D.M. Microarrays of cells expressing defined cDNAs. *Nature* **411**, 107–110 (2001).
3. Mousses, S. *et al.* RNAi microarray analysis in cultured mammalian cells. *Genome Res.* **13**, 2341–2347 (2003).
4. Silva, J.M., Mizuno, H., Brady, A., Lucito, R. & Hannon, G.J. RNA interference microarrays: high-throughput loss-of-function genetics in mammalian cells. *Proc. Natl. Acad. Sci. USA* **101**, 6548–6552 (2004).
5. Yoshikawa, T. *et al.* Transfection microarray of human mesenchymal stem cells and on-chip siRNA gene knockdown. *J. Control. Release* **96**, 227–232 (2004).

6. Vanhecke, D. & Janitz, M. High-throughput gene silencing using cell arrays. *Oncogene* **23**, 8353–8358 (2004).
7. Federico, M. (ed.). *Lentiviral Gene Engineering Protocols* (Humana Press, Totowa, New Jersey, 2003).
8. Stewart, S.A. *et al.* Lentivirus-delivered stable gene silencing by RNAi in primary cells. *RNA* **9**, 493–501 (2003).
9. Rubinson, D.A. *et al.* A lentivirus-based system to functionally silence genes in primary mammalian cells, stem cells and transgenic mice by RNA interference. *Nat. Genet.* **33**, 401–406 (2003).
10. Guertin, D.A. & Sabatini, D.M. An expanding role for mTOR in cancer. *Trends Mol. Med.* **11**, 353–361 (2005).
11. How, S.E. *et al.* Polyplexes and lipoplexes for mammalian gene delivery: from traditional to microarray screening. *Comb. Chem. High Throughput Screen.* **7**, 423–430 (2004).
12. Sarbassov, D.D. *et al.* Rictor, a novel binding partner of mTOR, defines a rapamycin-insensitive and raptor-independent pathway that regulates the cytoskeleton. *Curr. Biol.* **14**, 1296–1302 (2004).
13. Naldini, L. *et al.* In vivo gene delivery and stable transduction of nondividing cells by a lentiviral vector. *Science* **272**, 263–267 (1996).
14. Inaba, K. *et al.* Generation of large numbers of dendritic cells from mouse bone marrow cultures supplemented with granulocyte/macrophage colony-stimulating factor. *J. Exp. Med.* **176**, 1693–1702 (1992).